Performance analysis of gas-liquid cylindrical cyclone (GLCC) separator with an inclined and perforated wall

HUANG Shanfang[1,*] WEN Yiqian[2] WANG Dong[3]

[1]*Department of Engineering Physics, Tsinghua University, Beijing 100084, China*

[2]*Shandong Electric Power Engineering Consulting Institute Corp. Ltd, Ji'nan 250013, China*

[3]*School of Energy and Power Engineering, Xi'an Jiaotong University, Xi'an 710049, China*

Abstract As primary separators in pressurized water reactors (PWRs), cyclone separators separate most of the water from vapor-water two-phase mixture, which is important to the safety and economics of nuclear power plants. To improve the performance of cyclone separators, we tested new structures in this study, e.g. porosity and inclined angle of the separator wall. Under different structures, separation efficiency and pressure drop were studied theoretically and experimentally. Results show that each of the structural parameters has an effect on separator performance, but none of the trends is monotonically in experimental ranges. Besides separator structures, the comprehensive performance is also determined by flow patterns. From segregated to homogeneous flow, the separation ability decreases. The separation efficiency is about 5% higher at 20° inclined angle when the superficial velocities are 0.012 and 16 m·s^{-1} for the liquid and gas, respectively. The separation efficiency is only 91% without an impeller, while it is up to 100% at the same superficial velocities of air and water, 16 and 0.015 m·s^{-1}, respectively. Based on the study, it is promising to understand deeply the separation mechanism and further to provide data for designing large-scaled separators for advanced pressurized water reactors.

Key words Cyclone separator, Two-phase flow, Separation efficiency

1 Introduction

Gas-liquid two-phase separation is encountered in many industries, e.g. nuclear, chemical and petroleum engineering. It is especially important to steam generator in nuclear power plants, determining the safety and economics. The primary separator is a cyclone separator, where water is removed from vapor-water two-phase mixture. The separation process is governed by gravity and centrifugal effect simultaneously. Many investigations have been carried out on gravity separation[1-4] and centrifugal separation[5-8], respectively. However, the latter was more predominant and has been paid most attention.

Concerning centrifugal separation, many investigations focused on the effects of structural and operational parameters. Movafaghian and Mohann[6] studied the hydrodynamics, and obtained many valuable experimental data, based on which separation models were built. In the experimental ranges, different structural parameters were varied, including vane angles, different hub diameters, and vane number. Results showed that separation ability was heavily dependent on vane angle, but less on hub diameter or vane number. Penga *et al.*[7] specially studied the effect of vortex end, and tried to understand the mechanism of centrifugal cyclone from vortex moving. Wang *et al.*[8] broadened the range of separator application by adjusting the liquid level and pressure. Ahn *et al.*[5] studied centrifugal cyclone separation under low gravity conditions, and found that gravity effect varied against operational conditions. Additionally, flow pattern was crucial to GLCC. Green and Hetsroni[9] presented the requirements for GLCC that flow pattern

Supported by National Natural Science Foundation of China (No. 51006068) and Science and Technology on Reactor System Design Technology Laboratory, Nuclear Power Institute of China.

* Corresponding author. *E-mail address:* sfhuang@mail.tsinghua.edu.cn

Received date: 2012-11-7

be standard annular with uniform film thickness over the pipe wall, and that no water droplets should be entrained in the gas core. Creutz and Mewes[10] studied centrifugal separation in intermittent flows by driving the impeller with an electrical motor. Recently, Kotaoko *et al.*[11] studied the separation efficiency as well as pressure drop in annular flows by varying the impeller structures. The results showed that the impeller structure was important to the performance of centrifugal separators. Further, the parameters related to the structure should be optimized to obtain integrative optimization in separation efficiency and pressure drop.

The above investigations were mainly experiments, and still some tried to disclose the mechanism of GLCC separation by numerical simulations. Many efforts were made in Delft University of Technology in 1970s and 1980s[12-14]. Since then, numerical simulation has always been a focus[15-18]. The numerical simulation helped to connect flow field with separation process, but CFD is not powerful enough to discarding experiments completely.

For engineering applications, researchers tried to provide direct data and models. Green and Hetsroni[9] reviewed typical GLCC separators in different companies, e.g. Curtis-Wright, Westinghouse, GE, KWU, and CE. A new centrifugal separator proposed in Italy should be particularly mentioned[19]. New swirl vane was devised with a conical perforated riser, and other structures were also optimized such as riser perforation, skimmer, tangential slots and outlet nozzle. The new separator was then manufactured and tested with a full scale.

To the new structures, inclined angle and perforated wall, Huang *et al.*[20] carried out initial researches on separation efficiency and pressure drop, but it was lack of systemic analysis to the comprehensive performance. Additionally, there are some misunderstandings to the performance of the separator in Huang *et al.*[20].

There have been many investigations on cyclone separation and some even specially aiming at nuclear power plant, but many drawbacks are still existing which restrict the development of large-scaled GLCC separators: it is lack of studies on separation process and on the working mechanism. The experimental data are not effectively analyzed and correlated; parameter ranges are not wide enough to cover large-scaled nuclear power plants. Since the separator design is mainly dependent on experimental data, and new experiments therefore are indispensable in the future; additionally, traditional research methods help little to disclose the process and the mechanism, so new methods should be developed.

Since the new structure mentioned by Mauro *et al.*[19] may be promising to be used in larger primary separators, our aim is to analyze the mechanism clearly in this study. Based on the experimental study in Ref.[20], this paper theoretically describes the separation process and then assesses the functions of new structures, including impeller, perforated wall and inclined angle. In each stage, the flow mechanism was studied in detail. After the theoretical expressions, the experiments will be presented to see the separator performances under different structures. Factors related to structure and operation are analyzed how to have effects on the separation process.

2 Theoretical analyses

Figure 1 shows a sketch of centrifugal separator with new components, i.e. inclined and perforated wall. When two-phase flow is passing through an impeller, it will be driven to rotate. Liquid with a higher density prefers to move to the wall due to centrifugal force. Then the liquid penetrates into the holes in the perforated wall to form continuous water layer, realizing the two-phase separation. In this section, we first describe the separation process, and then analyze how the factors related to separator structure and operational conditions affect the process. The new structures will be particularly considered.

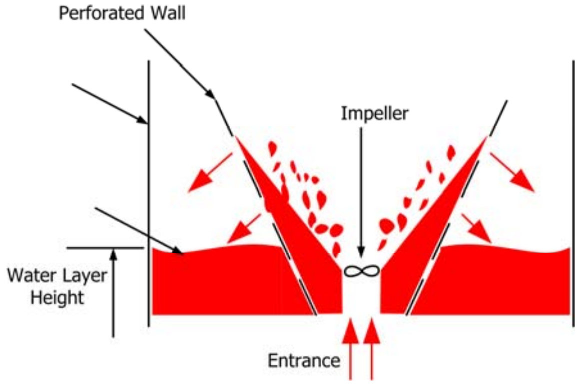

Fig.1 Separation process with new structures.

The process is decomposed into three stages, passing an impeller, moving to the pipe wall, and through the perforated wall.

2.1 Passing an impeller

When fluid enters a separator with a velocity along the axis, v_0, the velocity will be changed into three branches, v_a, v_t and v_r, in axial, tangential, and radial directions. For a spherical droplet with a diameter of d and a mass of m, the kinetic energy variation is therefore

$$\Delta E = -\frac{1}{2}m({v_a}^2 + {v_t}^2 + {v_r}^2 - {v_0}^2) \tag{1}$$

On the one hand, it is expecting to reduce ΔE, since it is a main part of total pressure drop in the separation process. On the other hand, pressure drop is inevitable since centrifugal separation is adopted to improve the separation efficiency. Many factors determine the energy variation, ΔE, together such as the shape, size and rotation state of the impeller. Huang *et al.*[20] compared pressure drop in a cyclone with a rotational and a fixed distributor, respectively. The results showed that pressure drop was much lower with a rotational distributor than with a fixed one. The function of the impeller is to rectify flow pattern into standard annular[9]. Theoretically, the liquid film is evenly distributed over the pipe wall without droplets entrained in the gas core.

2.2 Traversing the separator

After the impeller, a typical droplet will move upward along a helical path. Fig.2 shows the separation mechanisms in three coordinates.

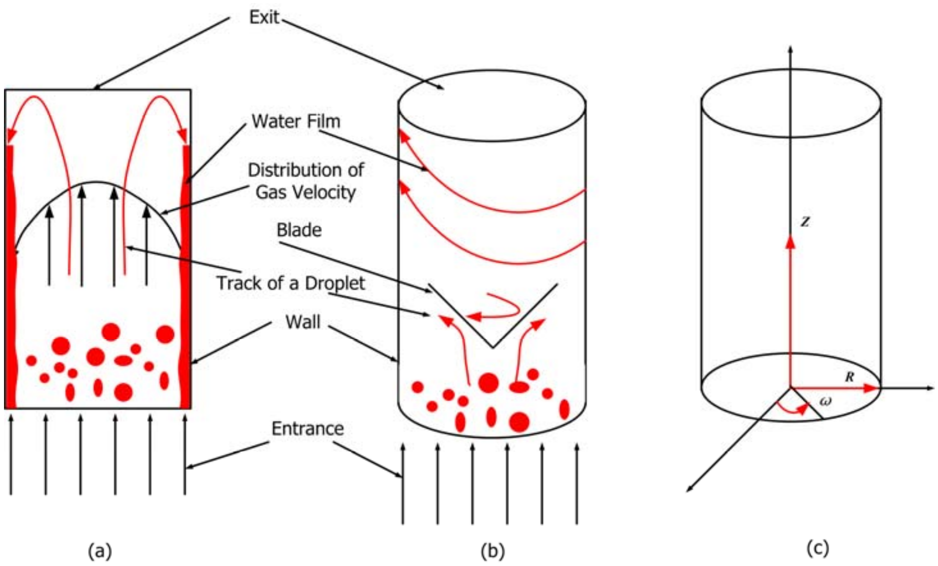

Fig. 2 Separation process. Gravity separation (a), Cyclone separation (b) and Cylindrical coordinates (c).

1) Axial

In axial direction, gravity effect governs the separation process[4]. Fig.3 shows a force balance of a droplet.

$$ma = B + F - mg \tag{2}$$

where

$$B = \rho_G V g \tag{3}$$

$$F = \frac{1}{2}C_D \Delta v^2 \rho_L A \tag{4}$$

$$mg = \rho_L V g \tag{5}$$

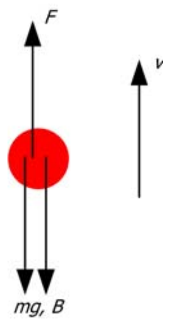

Fig.3 Force balance of a droplet.

The direction of friction, F, is positive or negative corresponding to the climbing and falling stage, respectively. From Eq.(2), the droplet prefers to be entrained into the gas and taken out of the separator as gas velocity increasing. Obviously, separation became worse when droplet size or two-phase difference reducing. Additionally, two-phase distribution has also important effect on separation ability. Separation ability becomes weak as flow pattern changes from segregated to homogeneous.

Qualitatively, an extreme is that the droplet is directly entrained out of the separator due to the big friction from gas with a big velocity. For most cases, droplet moves up and down since the friction is not big enough. In the falling stage, the droplet prefers to approach the wall instead of the center in the separator. The droplets will collide with each other and coalesce. When the coalesced droplet is big enough, it will stick to the separator wall, realizing gravity separation. For a given separator, it is expecting to prolong the staying time in the separator to improve separation efficiency.

2) Circumferential

Figure 4 shows a droplet moving in circumferential direction including in the separator and through a hole. Gravity separation efficiency is generally lower than centrifugal separation efficiency. For the latter, the governing equation in circumferential direction is

$$ma = m\frac{v^2}{R} \tag{6}$$

The separation wall is inclined with an angle of θ between the wall and the vertical direction, so the horizontal distance between a droplet and the separator wall was extended to $R+H\cdot\text{tg}\theta$, as shown in Fig.4(a). Therefore, Eq.(6) can be replaced by

$$ma = m\frac{v^2}{R + H\text{tg}\theta} \tag{7}$$

Since the centrifugal acceleration is reduced, the separation ability is weakened. This is consistent with the practical applications[19]. We set a positive θ in this study because we wanted to compare theoretically the effect of positive and negative angle on separation efficiency. As an example, when the angle θ is positive, the flow channel area will be amplified, so the superficial velocity of air and water decreases. Therefore, the gravity separation effect is enhanced, while centrifugal effect is weakened.

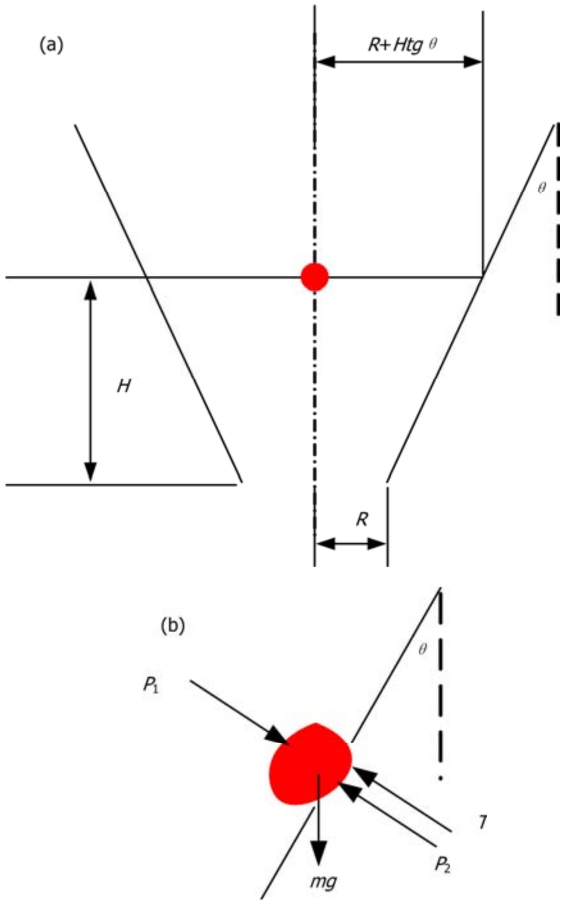

Fig.4 Moving process of a droplet. In the separator (a) and through a hole (b).

3) Radial

As to radial velocity, it helps to reduce the moving time to the separator wall. In the radial direction, the time is

$$t(r) = \frac{R + H\text{tg}\theta}{{v_r}^2} \tag{8}$$

As θ increasing, the time to reach the wall increases, increasing the probability of being entrained by air.

2.3 Through the perforated wall

When the droplet reaches the perforated wall, it will relapse into the continuous water layer and will further go through the hole in the inclined wall as shown in Fig.4(b). Many factors related to separator structure and water parameters determine the process for the droplet to drill through the perforated wall. If the following inequation is satisfied, the droplet will succeed in drilling through the hole.

$$\Delta PA + G\sin\theta > T + F_h \tag{9}$$

In Eq.(9), ΔP is pressure difference on the two sides of the hole. ΔP is determined by many operational parameters, e.g. water layer height and system pressure. T is a force due to surface tension σ; and F_h is friction through the hole.

The function of the perforated wall is to absorb water to avoid repeated collision and entrainment between gas core and water film over the surface of the separator. This helps to increase separation ability. When the hole is too big, gas will also be able to enter it, resulting in the disability in separation. On the other hand, water droplet will be rejected when the whole size is too small. To improve the separation ability, the size and shape of the holes should be optimized.

Since separated gas will enter the secondary separator after the primary separator, the mechanical energy consumption should be minimized. On the contrary, the liquid kinetic energy is expected to be used up. For a given separator, many operational parameters have effect on separation ability such as two-phase flow rates and system pressure. When the total mixture flow rate increases, the separation efficiency will generally decrease. Therefore, high-efficiency separator should be developed to meet the demand of large-scaled nuclear power plants of 1400 and even 1700 MW[8]. For a given separation load, the two-phase distribution in the separator, flow pattern, mainly determines the performance. To increase separation efficiency, Green and Hetsroni[9] required theoretically that the rectified flow pattern after the impeller be standard annular without droplets entrained in the gas core. Additionally, pressure has deep-seated effect on separator performance. When system pressure increases, the differences become smaller in two-phase parameters, such as surface tension, density, viscosity, and so on.

To obtain the separator performance, experimental work was carried out with new structures in air-water two-phase flows.

3 Experimental setup

3.1 Flow loop

Figure 5 shows an experimental setup, air-water two-phase flow loop used in this study. Air was supplied by a compressor to the mixer. The volumetric was metered by a Vortex flow meter made by Yokogawa Company, with an accuracy of ±1%. An inverse U-typed pipe, up to 2.5-m height, helped to prevent water from flowing back to the air loop. A pump drove water into the mixture and the flow rate was metered by two orifice flow meters for different ranges. After the mixer, the air-water two-phase flow flowed into a horizontal pipe, with a length of 8 m, before entering a vertical separator. After separation, air was vented directly to the atmosphere, whereas the entrained water was collected and metered. The time-averaged flow rate of the collected water was weighed by a platform balance. For the sake of observation, the whole test section, including the separator system and pipe, was made of transparent resin.

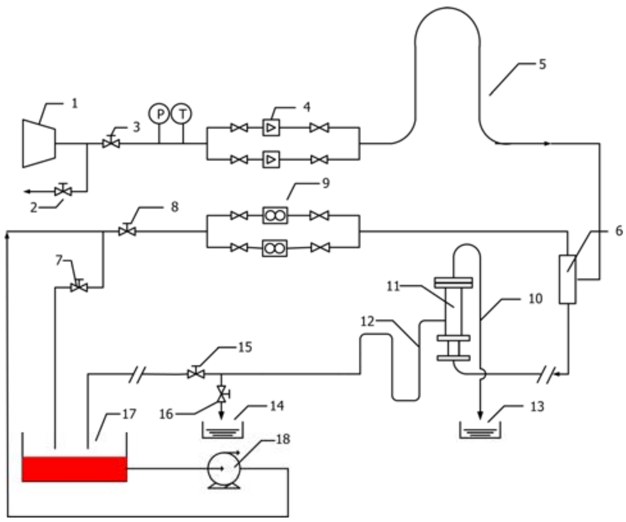

Fig.5 Air-water two-phase flow loop.

1 Compressor, 2 Air bypass valve, 3 Air regulating valve, 4 Vortex flowmeter, 5 Inversed U-typed pipe, 6 Mixer, 7 Water bypass valve, 8 Water regulating valve, 9 Orifice flowmeter, 10 Downcomer, 11 Gas-liquid separato, 12 U-typed water envelop, 13 and 14 Water barrel, 15 and 16 Ball valve, 17 Water tank, and 18 Water pump.

Three positions were set for pressure measurements, P_1, P_2 and P_3. System pressure was metered at P_1 with a pressure transducer, type of ST 3000. A pressure drop transducer placed between P_2 and P_3 was used to meter pressure drop in the separation process. The accuracy of pressure and pressure drop was within ±0.5%.

To observe the separation process, a digital high-speed camera was used, which was the same as that used in Zheng and Che[21]. From the video, we can observe the tracks of liquid droplets.

The experiments were conducted with low pressure and temperature, ranging of 0.1−0.15 MPa and 15−40°C. The superficial velocity of air and water was J_G=1−45 m·s^{-1} and J_L=0.005−0.060 m·s^{-1}, respectively.

3.2 Test sections

Different structures were tested in this study related to inclined angle and porosity. Fig.6 shows a process of two-phase separation. Two-phase mixture entered the separator from the bottom along the dashed line. In the separator, two-phase mixture was separated by gravity and centrifugal force simultaneously. After separation, single-phase water leaked to a single-phase water loop from the perforated wall, while air rose up to the top of the separator. To avoid that air was entrained into separated water, a U-shaped pipe was used in the water branch.

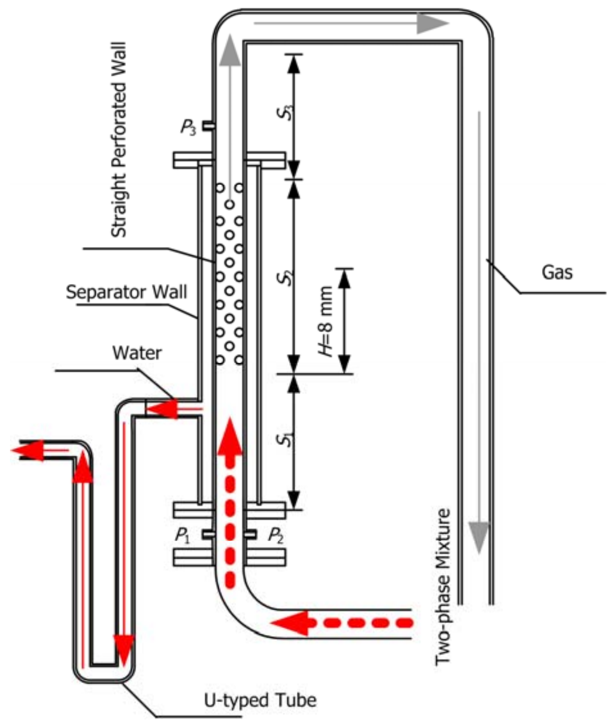

Fig.6 Separation process.

A separator can be divided into three parts, S_1, S_2, and S_3, corresponding to entrance, separation and exit, respectively. The length of Region S_1 was 32 cm. In the experimental ranges, the perforated wall was 50 mm and 30 mm in diameter at the bottom. In either case, the diameter of the separator chamber was fixed at 80 mm.

Figure 7 shows a typical perforated pipe, which was the core of the separator. A decussation made from sheet iron was placed at the entrance of the separator to rectify flow pattern. Above the decussation, there was an inclined wall with holes evenly distributed over the wall. In the experimental ranges, the inclined angle was 0°, 6°, 10° and 20°, respectively. For different inclined angles, the ratio of the whole area to that of the whole pipe was fixed at 15%.

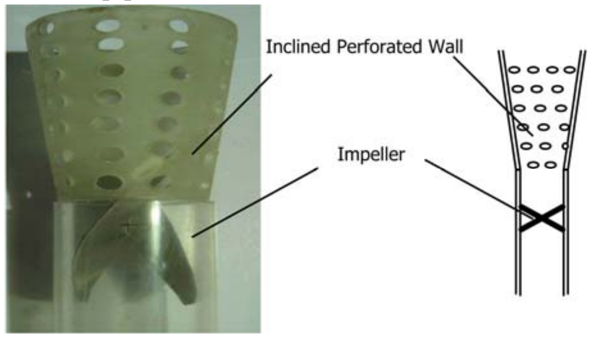

Fig.7 A typical separation structure.

In this study, since no air was assumed to be introduced into the single-phase water loop, separation efficiency can be defined from water side:

$$\eta = \frac{m_1}{m_0} \times 100\% \tag{15}$$

where m_0 and m_1 was water flow rate supplied to the system and separated in the single-phase water loop, respectively. The difference between them was the water entrained in the single-phase air after separation.

4 Results and discussion

In the experimental ranges, we present the separation performance from visual observations and separation efficiency.

4.1 Observation to two-phase separation

The separation process was very complex, but we can disclose qualitatively the mechanism by observing water droplet distributions. Table 1 summarizes the behaviors of two phases under different conditions without a decussation at the entrance. Water superficial velocity was constant, but the gas superficial velocity increased from case 1 to case 3.

In case 1, the liquid droplet jumped up and down in Region S_1, and continuous water layer accumulated. We could hardly observe rotational droplets, indicating that gravity effect was predominant in two-phase separation. As a whole, for gravity separation, water droplets preferred to approach the pipe wall in the falling stage. In Region S_2, only when water height was over a critical value, can water leak from the perforated wall. This increased P_1 in Eq.(9), helping to improve separation ability. There was no water entrained in Region S_3 and above, since the friction between water and air was so weak that the gravity cannot be balanced. Therefore, the separation efficiency was 100%.

Table 1 Water droplet tracks under gravity separation (D=50 mm, J_l= 0.015 m·s^{-1}, θ=0°)

Case	J_g	S_1	S_2	S_3	Exit
1	2.3	Bubble ring slowly	Water film moving up and down, some water droplet shooting out of the holes	×	×
2	4.2	Fountain	Water film moved up and down, some water droplet shooting out of the holes	Discrete water film covered the wall	×
3	10.9	Annular flow	Annular flow with the thickness being thinner from the bottom to the top, water shooting becoming weak	Few thread water droplet over the wall	Some water droplets were entrained in air

In case 2 when air flow rate increasing, the performance of water droplets were similar to case 1 but with some differences. In S_1, fountain occurred intermittently. In Region S_2, water became thinner and even was torn into discrete film sticking to the wall in climbing and falling stages. Some water droplets were entrained to Stage S_3 and even outside of the separator, but the separation efficiency was still 100%.

When gas velocity increased further in Case 3, flow pattern in Region S_1 became annular. More water droplets were entrained in S_2 and S_3, the separation decreased. When gas velocity was big enough, water stopped moving up and down and was directly entrained outside of the separator. At the same time, continuous water film was broken into several discrete sections.

The probability that water droplets shot out of the holes decreased as a function of water layer height in the perforated wall. To describe the separation process quantitatively, we counted the jumping times that water layer moved up and down. Three numbers were defined, N, N_0, and N_1. N was the total times in the whole S_2 region; N_0 was the jumping times beyond a height from the root of S_2 , e.g. H=8 mm as shown in Fig. 6; and N_1 was the times below H. Fig.8 shows N, N_0 and N_1 within the same period of three minutes.

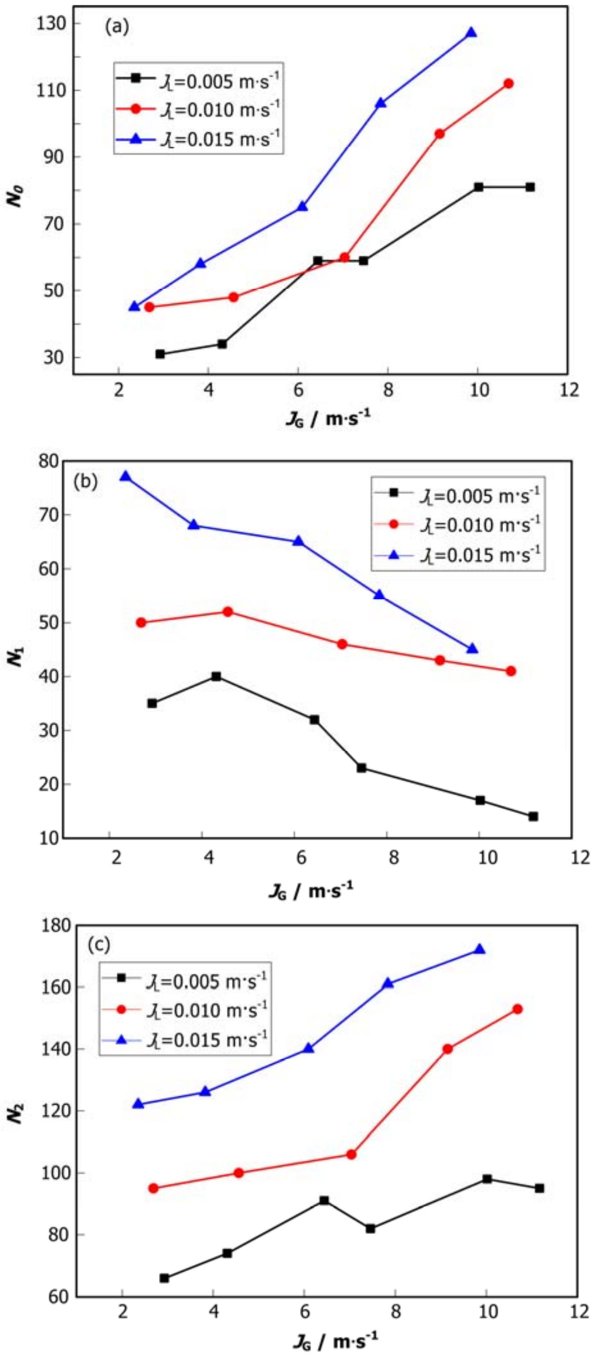

Fig.8 Jumping times. N_0(a), N_1 (b) and N_2(c).

From Fig.8(a), with a constant J_L, N_0 increases as a function of J_G because the entrainment ability is enhanced. At the same time, when liquid flow rate increases, N_0 has a similar trend. However, N_0 is more influenced by J_G. To satisfy in Eq.(9), water layer height must be higher, corresponding to a bigger N_0. Conversely, N_1 decreases against gas velocity. As gas velocity increases, the friction between gas and liquid becomes larger to enhance the entrainment ability, and further weakens the separation efficiency.

Comparing gravity and centrifugal separation, the only difference in separator structure is the existing or not of a decussation at the entrance to the separator, but the separation mechanisms are completely different. When an impeller appears, flow pattern is rectified to annular flow more or less. Fig.9 shows the flow pattern rectification above Region S_3. When gas velocity is low in Case 1, the centrifugal effect is very weak, the impeller is more a throttler than a cyclone.

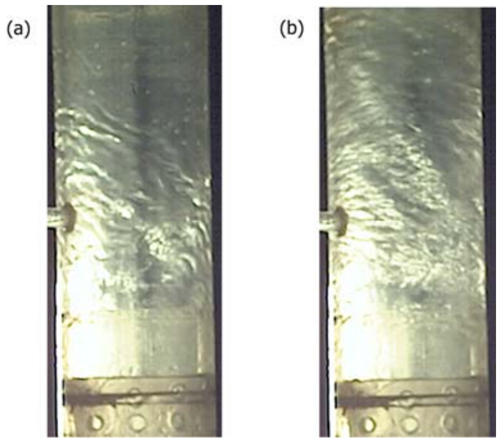

Fig.9 Flow pattern rectification with a decussation (θ=10°, J_L=0.012 m·s^{-1}). J_G=27.772 m·s^{-1}(a) and (b) J_G=34.793 m·s^{-1}.

When gas velocity increases, e.g. j_G=8 m·s^{-1}, centrifugal effect becomes important. Annular flow pattern appeared with a lower gas velocity, and water shoots out of the perforated wall more easily. The separation efficiency is much higher than that without an impeller. If gas velocity is over a critical value, the separation efficiency is lower than 100%. The residual water after the perforated wall is along a helical annular flow. As gas velocity further increases, the torsion becomes obvious. As a whole, water film in the annular flows becomes thinner and thinner from the bottom to the top by leaking from the perforated wall gradually. As inclined angle is increasing, separation ability is observed to be weakened. This validated the theoretical analysis in Section 2.

4.2 Separation efficiency

Separation efficiency is determined by many factors related to structural and operational conditions, such as impeller shape, size and distribution of holes over the perforated wall, inclined angle of separator wall, and flow pattern. The effects of the parameters were tested one by one in this study.

4.2.1 Impeller

To compare the effect of an impeller on separation efficiency, we carried out experiments in a straight perforated pipe with and without an impeller, respectively, as shown in Fig.10. It should be noted that the results in Fig.10 are the benchmarks of the new structures to be discussed later. The diameter of the perforated pipe is set at 30 mm and 50 mm, respectively. The separation efficiency is only 91% without an impeller, while it is up to 100% with the impeller at the same superficial velocities of air and water, 16 and 0.015 m·s^{-1}, respectively. With an impeller, water prefers to be thrown to the pipe wall due to the centrifugal force. According to Eq.(6), the centrifugal force is qualitatively much higher for the air than for the water. Therefore, the water is easy to be separated from the perforated wall. Although the impeller helps to increase the separation efficiency, the impeller structure needs also optimization concerning the pressure drop across the impeller.

As the gas velocity increases with a constant liquid velocity, the separation efficiency decreases as shown in Fig.10(a). However, there are opposite trends in local regions due to flow pattern transition. As gas velocity becomes higher, flow pattern was changing from being segregated to homogeneous. The separation mechanism may therefore be varying due to the different flow patterns. Additionally, the separation efficiency is higher in the 30 mm-diameter pipe than in the 50 mm-diameter one. This was also due to flow pattern variation. In pipes with different diameters, flow pattern boundaries are different, resulting in the contravention between efficiency curves.

Water superficial velocity has a complex effect on separation process. When water superficial velocity is increasing, gas cannot provide enough friction to take water out of the separator. Therefore, the separation efficiency becomes higher. Conversely, when water velocity is high enough, water droplet itself can directly jump out of the separator, reducing the separation efficiency. As a whole, separation efficiency is higher in a smaller diameter and a lower liquid velocity.

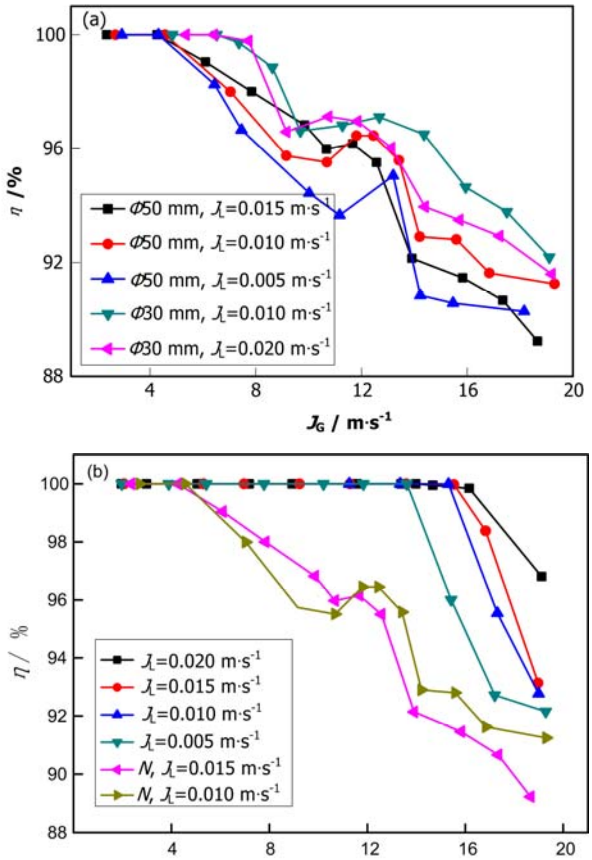

Fig.10 Separation efficiency in straight perforated pipe. Without an impeller (a) and comparison the effect of an impeller with a diameter of 50mm ("N" means there was not an impeller at the entrance) (b).

To compare the effect of the impeller, Fig.10(b) presents simultaneously the efficiencies with and without an impeller. For the former, the critical gas velocity corresponding to complete separation has been postponed from 4 m·s^{-1} to 14 m·s^{-1}. Flow pattern is rectified to annular flows more or less, and centrifugal effect is therefore introduced to improve the separation efficiency. Under the obstruction from the impeller, axial velocity was sharply reduced, but radial and circumferential velocity was created, which can remarkably enhance separation efficiency. Therefore, the impeller can intensify separation efficiency obviously by centrifugal effect.

4.2.2 Cone

Figure 11 shows the separation efficiency in 6° and 20° pipes without an impeller. The trends are similar under different liquid velocities that it decreases as a function of gas velocity but with a trough within 10−15 m·s^{-1}. The curve can be divided into three stages, marked by I, II and III, where the separation mechanisms are different from each other in the different regions.

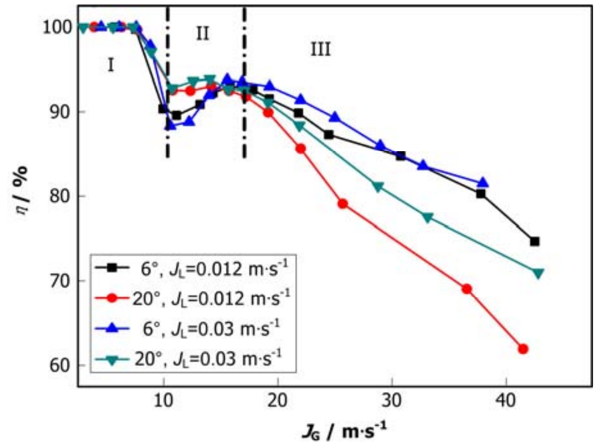

Fig.11 Separation efficiency in 6° and 20° pipes without an impeller.

In stage I, since gas turbulence is very weak and gravity separation was predominant, the separation efficiency is very high. As the gas superficial velocity increases, the flow patterns are plug, slug, and annular flows. When the gas superficial velocity is very low with a flow pattern of plug, the separation is quite high due to the gravity effect.

In stage II, gas rises from continuous water as a big bubble, which is like a fountain. The separation efficiency increases against gas velocity. Gas and liquid pass the separator alternately with a slug flow, so it is difficult to separate water from gas completely, especially when the liquid slug is passing. As the inclined angle is becoming larger, the separation efficiency becomes bad. Both velocities of air and water decrease as a function of inclined angle, and two-phase flow tends to be heterogeneous. Friction pressure drop decreases and further decreases the separation efficiency.

In stage III, the predominant flow pattern is annular with a big gas superficial velocity, and the effect of inclined angle is opposite to that in stage II. The thickness of the water film surrounding the gas core becomes thinner as gas velocity increase, and more and more water droplets are entrained into the gas core with a limiting flow pattern, namely mist flow. Therefore, the separation ability becomes weak. In the third region, the flow pattern is annular and most water is located at the surface of the pipe wall. According to the separation mechanism shown in Fig.2, the water is easy to be separated in annular flows.

When the inclined angle is 6°, the separation efficiency would be 92% at the superficial velocities of 0.015 $m\cdot s^{-1}$ and 18 $m\cdot s^{-1}$ for water and air, respectively. It is about 3% higher that without the inclined angle as shown in Fig.10. The velocities of the air and water decrease in the separation chamber with an inclined angle, and the gravitational effect is predominant. Under this condition, the Eq.(9) is easy to meet leading to a higher separation efficiency for the 6° case. In contrast, the separation efficiency decreases when the inclined angle is 20°. Under this condition, the secondary mixing occurs between air and water, which leads to a lower separation efficiency. The results under 6° and 20° show that the inclined angle needs optimization.

Figure 12 shows the separation efficiency with an impeller and a cone wall. As gas velocity increases, the separation ability turns out to be weak, which is different from that without an impeller. The separation ability decreases against the inclined angle, but the trends are different in 6° and 10° pipes. For the former, separation efficiency is higher than 98% even when gas superficial velocity is up to 44 m/s. The deterioration is remarkable in the 10° and 20° pipes.

An impeller can intensify separation efficiency not only in straight pipes, but also in inclined ones. As an example, in 20° inclined pipes, the separation efficiency is 15% higher with an impeller than without it for the same superficial velocities of air and water, 36 $m\cdot s^{-1}$ and 0.03 $m\cdot s^{-1}$, respectively. Compared with an impeller, the inclined angle effect is much weaker to separation efficiency.

Figure 13 shows the separation efficiencies under different inclined angles. For any cases, an impeller is helpful to increase separation efficiency sharply, by adjusting the flow pattern into annular. The separation efficiency profiles are together determined by the inclined angle, the impeller and the perforated water. For each inclined angle, 6° or 20°, the separation efficiency is higher with an impeller than without the impeller. As an example, the separation efficiency is about 5% higher when the superficial velocities are 0.012 and 16 $m\cdot s^{-1}$ for the liquid and gas, respectively.

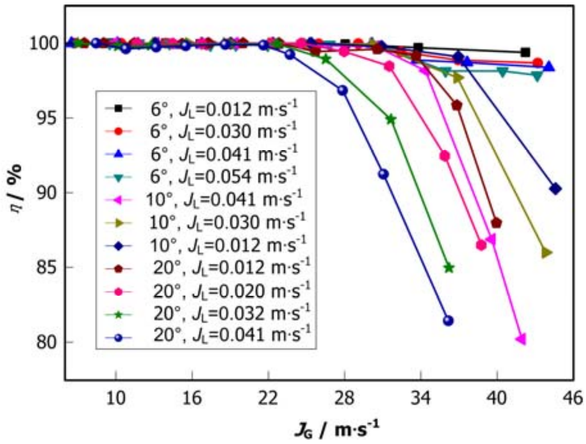

Fig.12 Separation efficiency in 6°, 10°and 20°pipes with an impeller.

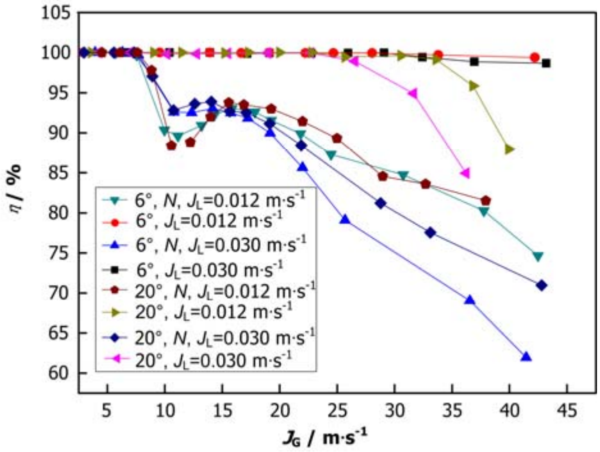

Fig.13 Effect of impeller on separation efficiency.

4.3 Future work

As operational parameters increase greatly in large-scaled power plant, e.g. China's Advanced Pressurized Water Reactor (CAP1400), the performance of primary separators may vary due to the differences in structure and operation. Further studies should focus on the performance of CAP1400's separator from engineering view. Parameters related to separator structures should be optimized to improve separation efficiency and to decrease pressure drop. Additionally, new structures may be adopted in design the separator, e.g. a rotational impeller.

5 Conclusion

Separation efficiency and pressure drop are important targets to reflect the performance of GLCC separators, e.g. a primary separator in steam generators. The separation process is determined by many factors related to structural and operational parameters. To verify the effect of the new structures, e.g. inclined angle and perforated wall, we present the separator performance theoretically and experimentally. The following conclusions may be drawn.

Separation process is governed by gravity and centrifugal effect simultaneously. By tracing a droplet, the process can be divided into three stages including passing the entrance, traversing the separator and drilling the perforated wall. The ideal condition is to use up liquid kinetic energy but to keep gas velocity.

An impeller can intensify the separation by introducing a centrifugal effect. For any inclined angle, 6° or 20°, the separation efficiency is higher with an impeller than without the impeller. As an example, the separation efficiency is about 5% higher at 20° inclined angle when the superficial velocities are 0.012 and 16 m·s^{-1} for the liquid and gas, respectively.

To a perforated wall, it enhances separation efficiency by consuming kinetic energy of liquid phases and sucking water film gradually in perforation process. When the inclined angle is 6°, the separation efficiency is 3% higher than that without the inclined angle decreases. In contrast, the separation efficiency is lower at 20° inclined angle.

Nomenclatures

a Acceleration (m/s^2)
d Diameter (m)
f Friction coefficient
m Mass (kg)
v Velocity (m/s)
A Hole area (m^2)
B Buoyancy (N)
F Friction (N)
J Superficial velocity (m/s)
R Radius (m)

Greek letters

θ Angle
σ Surface tension (N/m)
α Void fraction
ρ Density (kg/m^3)
μ Viscosity (Pa·s^{-1})
η Separation efficiency

Subscripts

A Axial direction
ac Acceleration
f Friction
fo Form
G Gravitational
R And radial direction
T Tangential direction
V Vapor
W Water
G Gas
L Liquid
TP Two-phase

References

1 Liu S. China Nuclear Technology Report, 1996.

2 Chen S H, Huang S Y, Zhao X X. J Huazhong Univ Sci Technol, 1997, **25:** 69–71.

3 Baker G, Clark W W, Azzopardi B J, *et al.* Chem Eng Sci, 2008, **63:** 968–976.

4 Yue D B, Xu Y D, Mahar R B, *et al.* Chem Eng J, 2007, **126:** 171–180.

5 Ahn H S, Tanaka K, Tsuge H. Sep Purif Technol, 2000, **19:** 121–129.

6 Movafaghian J A, Mohann J M R. Int J Multiphase Flow, 2000, **26:** 999−1018.

7 Penga W, Hoffmanna A C, Driesb H W A, *et al.* Chemical Engineering Science, 2005, **60:** 6919–6928.

8 Wang S, Mohan R S, Shoham O. J Energy Resour Technol, 2000, **122:** 85–192.

9 Green S J, Hetsroni G. Int J Multiphase Flow, 1995, **21:** 1−97.

10 Creutz M, Mewes D. Int J Multiphase Flow, 1998, **24:** 1057−1078.

11 Kataoka H, Matsubayashi T, Shinkai Y, *et al.* 8th International Conference on Nuclear Thermal-Hydraulics, Operation and Safety (NUTHOS-8). Shanghai, China, 2010.

12 Prints C A. Ph.D. Thesis, Delft University of Technology, 1974.

13 Van der Welle R. Ph.D. Thesis, Delft University of Technology, 1983.

14 Wisman R. Ph.D. Thesis, Delft Univ Technol, 1979.
15 Erdal F M, Shirazi S A. J Energy Resour Technol, 2006, **128:** 62−69.
16 Erdal F M, Shirazi S A, Shoham O. SPE 36645, SPE 71st Annual Meeting, Denver, CO, US, 1996.
17 Snyder D O, Spall R E. Phys Fluids, 2000, **12:** 603–608.
18 Xiang R B, Lee K W. Chem Eng Proc, 2005, **44:** 877–883.
19 Mauro G, Sala M, Hetsroni G. Nucl Eng Design, 1990, **118:** 179−192.
20 Huang S F, Wen Y Q, Wang D. Proceedings of the 19th International Conference on Nuclear Engineering (ICONE19), Paper43328, Chiba, Japan, 2011.
21 Zheng D, Che D. Int J Multiphase Flow, 2006, **32:** 1191–1218.